

Peculiarities of wave fields in nonlocal media

V.A.Danylenko¹ and S.I.Skurativskyi^{1, a)}

*Division of geodynamics of explosion, Subbotin institute of Geophysics,
NAS of Ukraine*

(Dated: 11 November 2021)

The article summarizes the studies of wave fields in structured non-equilibrium media describing by means of nonlocal hydrodynamic models. Due to the symmetry properties of models, we derived the invariant wave solutions satisfying autonomous dynamical systems. Using the methods of numerical and qualitative analysis, we have shown that these systems possess periodic, multiperiodic, quasiperiodic, chaotic, and soliton-like solutions. Bifurcation phenomena caused by the varying of nonlinearity and nonlocality degree are investigated as well.

PACS numbers: 74D10, 74D30, 37G20, 34A45

Keywords: nonlocal models of structured media; traveling wave solutions; chaotic attractor; homoclinic curve; invariant tori

^{a)}skurserg@gmail.com

In order to describe non-equilibrium media when the manifestations of intrinsic structure can not be ignored, we use hydrodynamic mathematical models. Information about relaxing processes and interactions between structural elements is incorporated in the dynamical equations of state (DES) which, unlike the local classic relations, now become nonlocal one in time and space. Using the symmetry reduction scheme, we obtain the autonomous dynamical systems describing the invariant wave solutions. By qualitative analysis methods, we show that the dynamical systems possess periodic, multiperiodic, and chaotic solutions obeying the Feigenbaum scenario. We study the quasiperiodic regimes and their bifurcations. We also reveal the existence of homoclinic trajectories of Shilnikov type and investigate the changes of homoclinic structures when the bifurcation parameters vary. Hidden attractors, hysteretic phenomena are discovered as well. As a result, depending on the chosen model for media, we classify the wave solutions and their bifurcations and show that spatio-temporal nonlocal models are promising for the describing of complicated wave regimes in structured media.

I. INTRODUCTION

Open thermodynamic systems attract attention of scientists by their synergetic properties, their ability to produce localized nontrivial structures and order. Description of such phenomena demands the creation of new and the refinement of already known mathematical models.

According to Refs. 1–3, using the methods of non-equilibrium thermodynamics and the internal variables concept⁴, the nonlinear temporally and spatially nonlocal mathematical models for non-equilibrium processes in media with structure have been constructed. In this report we present the results of investigations of wave processes in such media. To do this, we use the following hydrodynamic type system

$$\begin{aligned} \dot{\rho} + \rho u_x = 0, \quad \rho \dot{u} + p_x = \gamma \rho^m, \\ \frac{1}{\rho^2} \frac{\Gamma \varepsilon_r}{\tau_{TP}} \left\{ \left[-\rho_{xx} (1 + \mathbf{a}) + \frac{1}{\rho} (\rho_x)^2 (1 - \mathbf{a} \Gamma_{V0}) \right] + [-\ddot{\rho} (1 + \mathbf{a}) + \right. \end{aligned}$$

$$\begin{aligned}
& \left. + \frac{2}{\rho} \dot{\rho}^2 \left(1 - \frac{\mathbf{a}(\Gamma_{V0} - 1)}{2} \right) + \frac{1}{\tau_{TP}} \dot{\rho} (1 + \mathbf{a}) \right\} + \omega_0^2 \rho_0^{1-\Gamma_{V0}} \rho^{\Gamma_{V0}} - \\
-\omega_0^2 \rho_0 &= b(p - p_0) + b\tau_{TV} \dot{p} - \frac{\chi_{T0}}{\chi_{T\infty}} b\tau_{TV}^2 \ddot{p} - b\Gamma_{\varepsilon_r} \tau_{TV} \left(p_{xx} + \frac{\rho_x}{\rho} p_x \right), \tag{1}
\end{aligned}$$

where

$$\begin{aligned}
\mathbf{a} &= T_0 \alpha_{\infty} \Gamma_{V0} \left(\frac{\rho}{\rho_0} \right)^{\Gamma_{V0}+1}, \quad \omega_0^2 = \frac{bc_{S0}^2 \alpha_0 T_0}{\gamma_0}, \\
b &= \frac{\chi_{T0}}{\rho_0 \tau_{TP}^2}, \quad \chi_{T0} = \rho_0^{-1} c_{T0}^{-2} = \gamma_{\infty} \rho_0^{-1} c_{S0}^{-2};
\end{aligned}$$

c_{T0} , c_{S0} are the isothermal and adiabatic frozen velocities of sound; γ_{∞} is the frozen polytropic index.

Using the characteristic quantities t_0 , u_0 , ρ_0 , let us construct the scale transformation

$$\begin{aligned}
t &= \bar{t}t_0, \quad x = \bar{x}t_0u_0, \quad p = \bar{p}\rho_0u_0^2, \quad \rho = \bar{\rho}\rho_0, \quad u = \bar{u}u_0 \\
\sigma &= \frac{\Gamma_{\varepsilon_r} \tau_{TV}}{(t_0u_0)^2}, \quad \tau_{pT} = \tau_{TV} \frac{\chi_{T0}}{\chi_{T\infty}}, \quad \tau = \frac{\tau_{TV}}{t_0}, \quad h = \frac{\chi_{T0}}{\chi_{T\infty}} \tau^2, \\
\kappa &= \frac{\omega_0^2}{bu_0^2} = \alpha_0 T_0 \gamma_0 \left(\frac{C_{T0}}{u_0} \right)^2, \quad \chi = \frac{1}{\rho_0 u_0^2 \chi_{T\infty}} \equiv \left(\frac{C_{T\infty}}{u_0} \right)^2, \\
& \quad a = \delta n \rho^{n+1}, \quad \delta = T_0 \alpha_{\infty}, \quad \Gamma_{V0} = n,
\end{aligned} \tag{2}$$

which leads system (1) to the dimensionless form

$$\begin{aligned}
\dot{\rho} + \rho u_x &= 0, \quad \rho \dot{u} + p_x = \gamma \rho^m, \\
\sigma \chi \rho^{-2} & \left[-\rho_{xx} (1 + a) + \rho_x^2 \rho^{-1} (1 - an) \right] + \\
+h \chi \rho^{-2} & \left[-\ddot{\rho} (1 + a) + 2\dot{\rho}^2 \rho^{-1} (1 - 0.5a(n-1)) + \tau h^{-1} \dot{\rho} (1 + a) \right] + \\
+\kappa \rho^n &= p + \tau \dot{p} - h \ddot{p} - \sigma \left(p_{xx} + \rho_x p_x \rho^{-1} \right).
\end{aligned} \tag{3}$$

We would like to emphasize that system (3) can be regarded as an hierarchical set of submodels which are complicated by means of taking new effects into account. We thus are going to study the chain of nested models and classify their wave solutions using the methods of qualitative and numerical analysis.

The remainder of the report is organized as follows. In Sec.II we begin our studies from the simplified version of system (3) keeping the terms with the first temporal derivatives, then attaching the terms with the second temporal or spatial derivatives. The form of wave solutions and the description of techniques for their exploration are presented in detail. Sec.III is devoted to the spatially nonlocal model which is used for investigating of

the Shilnikov homoclinic structures whose existence and bifurcations are extremely important during chaotic regimes formation. The model incorporated both temporal and spatial nonlocalities are presented in Sec.IV. Generalizations of the previous models by means of introducing the third temporal derivatives and incorporating of physical nonlinearity are given in Sec.V and Sec.VI, respectively. For all models we derive invariant wave solutions and carry out the qualitative analysis of corresponding factor-systems.

II. WAVE SOLUTIONS OF THE MODELS WITH DES INCORPORATING THE SECOND TEMPORAL OR SPATIAL DERIVATIVES

To begin with, let us consider the simplest model with relaxation derived from (3) at $\delta = h = \sigma = 0$, $n = 1$. As has been shown in Refs. 4 and 5, the system

$$\dot{\rho} + \rho u_x = 0, \quad \rho \dot{u} + p_x = \gamma \rho, \quad \tau(\dot{p} - \chi \dot{\rho}) = \kappa \rho - p, \quad (4)$$

due to its symmetry properties⁶, admits the ansatz

$$u = U(\omega) + D, \quad \rho = \rho_0 \exp(\xi t + S(\omega)), \quad p = \rho Z(\omega), \quad \omega = x - Dt, \quad (5)$$

where D is the constant velocity of wave front, ξ determines a slope of the inhomogeneity of the steady solution (5). According to Ref. 5, solutions (5) are described by the plane system of ODE which possesses limit cycles and homoclinic trajectories.

If we incorporate the second temporal derivatives in the last equation of system (3), then the previous DES is generalized to the following one:

$$\tau \left(\frac{dp}{dt} - \chi \frac{d\rho}{dt} \right) = \kappa \rho - p - h \left\{ \frac{d^2 p}{dt^2} + \chi \left(\frac{2}{\rho} \left(\frac{d\rho}{dt} \right)^2 - \frac{d^2 \rho}{dt^2} \right) \right\}. \quad (6)$$

This model takes into account the dynamics of internal relaxation processes in more detail. As has been shown in Ref. 7, wave solutions (5) are described by the system of ODE with three dimensional phase space. This system possesses the limit cycles undergoing the period doubling cascade, and chaotic attractors.

Consider now the model with relaxation and spatial nonlocality

$$\tau(\dot{p} - \chi \dot{\rho}) = \kappa \rho - p + \sigma \left\{ p_{xx} + \frac{1}{\rho} p_x \rho_x - \chi \left(\rho_{xx} - \frac{1}{\rho} (\rho_x)^2 \right) \right\}. \quad (7)$$

Solutions (5) satisfy the following dynamical system

$$\begin{aligned}
U \frac{dU}{d\omega} &= UW, & U \frac{dZ}{d\omega} &= \gamma U + \xi Z + W(Z - U^2), \\
U \frac{dW}{d\omega} &= \{U^2[\tau(\gamma U + \xi Z - WU^2) + \chi\tau W + Z - \kappa] + \\
&+ \sigma[(\xi + W)(2U(\gamma - UW) + \chi W) + (UW)^2]\} [\sigma(\chi - U^2)]^{-1}.
\end{aligned} \tag{8}$$

This system has the fixed point

$$U_0 = -D, \quad Z_0 = \frac{\kappa}{1 - 2\sigma(\xi/D)^2}, \quad W_0 = 0, \quad \gamma = \xi Z_0/D \tag{9}$$

which is the only one lying in the physical parameter range.

We start from analyzing the linearized in the fixed point (9) system (8) with the matrix \hat{M}

$$\hat{M} = \begin{pmatrix} 0 & 0 & -D \\ \gamma & \xi & Z_0 - D^2 \\ A & B & C \end{pmatrix},$$

where

$$\begin{aligned}
A &= \frac{D\kappa\xi(2\xi\sigma - D^2\tau)}{Q\sigma(2\xi^2\sigma - D^2)}, & B &= \frac{D^2(1 + \xi\tau)}{Q}, & Q &= \sigma(\chi - D^2), \\
C &= Q^{-1} \left\{ \xi\sigma(\chi - D^2) - \frac{2D^2\kappa\xi\sigma}{D^2 - 2\xi^2\sigma} + D^2\tau(\chi - D^2) \right\}.
\end{aligned}$$

The well-known Andronov-Hopf bifurcation theorem⁸ tells us that periodic solution creation can take place if the spectrum of matrix \hat{M} looks as $(-\alpha; \pm\Omega i)$. This is so if the following relations hold:

$$\alpha = \xi + C > 0, \tag{10}$$

$$\Omega^2 = AD - B(Z_0 - D^2) + \xi C > 0, \tag{11}$$

$$\alpha\Omega^2 = \xi(AD - Z_0B) > 0. \tag{12}$$

The first two take on the form of inequalities imposing some restrictions on the parameters. The third one determines the neutral stability curve (NSC) in space $(D^2; \kappa)$ provided that the remaining parameters are fixed. For $\sigma = 0.76$, $\xi = 1.8$, $\tau = 0.1$, $\chi = 50$, it looks like a parabola with branches directed from left to right, see Fig.2a. Crossing the NSC from right to left, we observe the limit cycle appearance. Development of limit cycle at decreasing D^2 it is convenient to study by means of the Poincaré section technique^{9,10}.

Let us choose the plane $W = 0$ as an intersecting one and find coordinates of intersection points of phase curves which cross-sect the intersecting plane only in one direction. Plotting coordinate Z of the cross-section point along the vertical axis, and the value of the bifurcation parameter D^2 along the horizontal one, we will obtain the typical bifurcation diagrams (Fig.1). From the analysis of diagram Fig.1a we can see that while parameter D^2 decreases the development of the limit cycle coincides with the Feigenbaum scenario, followed by the creation of a chaotic attractor. Moreover, in the vicinity of the main limit cycle there are the hidden attractors (depicted in Fig.1a by the symbols I and II). These attractors can be visualized by the integrating of system (8) with special initial data only.

In Fig.1b we see the torus development at decreasing D^2 . According to the diagram, we can distinguish tori with densely wound trajectories and striped tori.

Doing in the same way, we get the two-parameter bifurcation diagram (Fig.2) which tells us that system (8) possesses the periodic, multiperiodic, quasiperiodic, and chaotic trajectories.

Such a complicated structure of the phase space of the system can be caused by homoclinic trajectory existence.

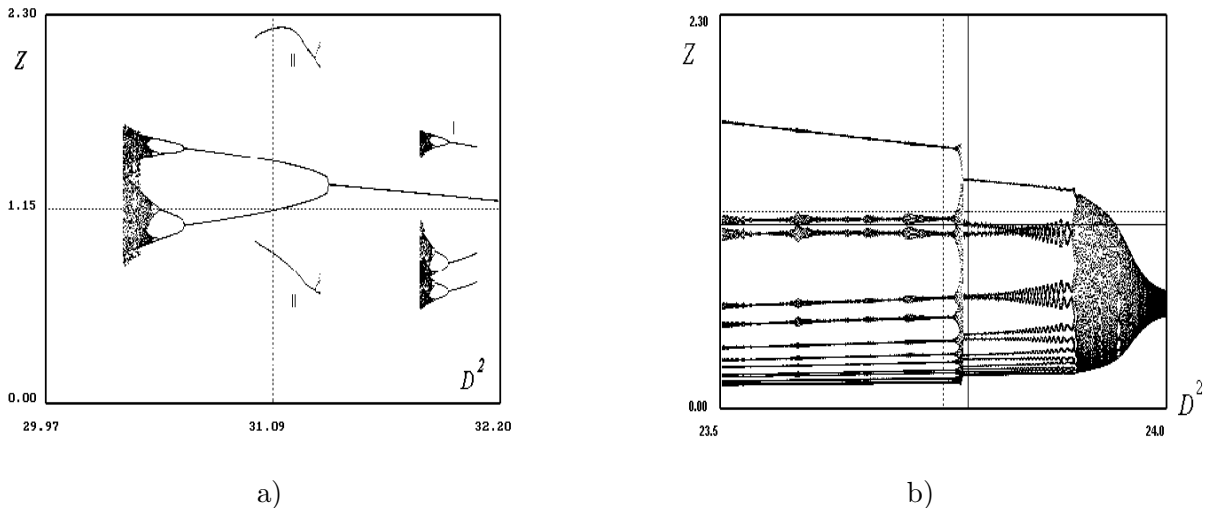


FIG. 1. Bifurcation diagrams of system (8) in plane (D^2, Z) , obtained for $\chi = \eta = 50$, $\xi = 1.8$, $\tau = 0.1$, $\sigma = 0.76$ and (a) $\kappa = 14$, (b) $\kappa = 1$.

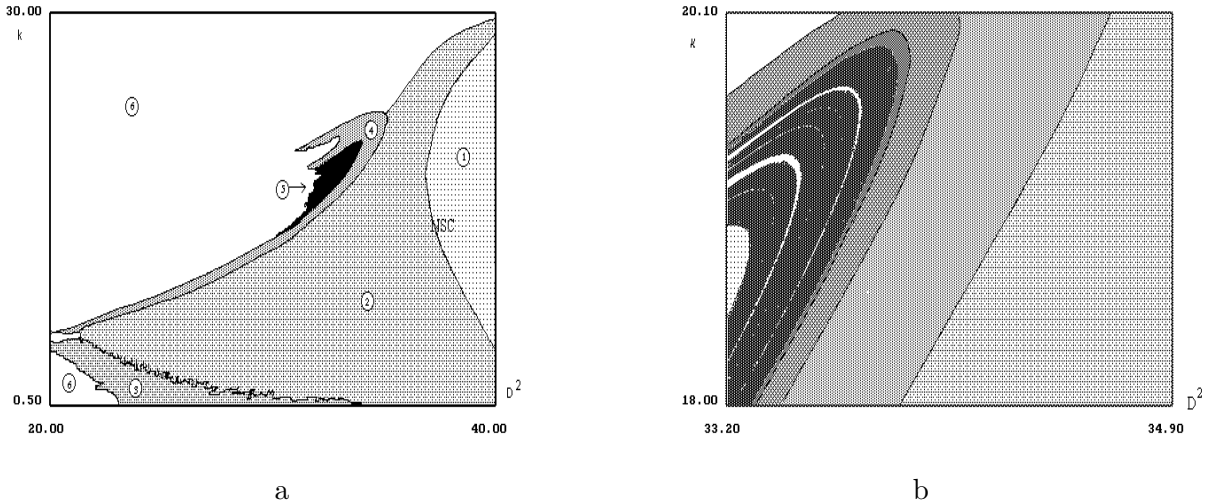


FIG. 2. Left: bifurcation diagram of system (8) in parametric space (D^2, κ) : 1 – stable focus; 2 – $1T$ -cycle; 3 – torus; 4 – multiperiodic attractor; 5 – chaotic attractor; 6 – loss of stability. Right: enlargement of part of the left figure: 6 – $3T$ -cycle.

III. HOMOCLINIC LOOPS OF SHILNIKOV TYPE AND THEIR BIFURCATIONS

First it worth noting that existence of homoclinic trajectories, i.e. loops consisting of the separatrix orbits of hyperbolic fixed point, plays a crucial role^{11,12} in the formation of localized regimes in the phase space of dynamical system.

For the present, the question on the existence of homoclinic trajectory of Shilnikov type^{8,13} in system (8) has been treated numerically.

We investigate a set of points of parameter space (D^2, κ) for which the trajectories moving out of the origin along the one-dimensional unstable invariant manifold W^u return to the origin along the two-dimensional stable invariant manifold W^s . In practice, for the given values of parameters κ, D^2 , we numerically define a distance (the counterpart of split function in Ref. 13, p.198) between the origin and point $(X^\Gamma(\omega), Y^\Gamma(\omega), W^\Gamma(\omega))$ of the phase trajectory $\Gamma(\cdot; \kappa, D^2)$:

$$f^\Gamma(\kappa, D^2; \omega) = \sqrt{[X^\Gamma(\omega)]^2 + [Y^\Gamma(\omega)]^2 + [W^\Gamma(\omega)]^2},$$

starting from the fixed Cauchy data $(0, 0, 0.001)$. Next we determine

$$\Phi(\kappa, D^2) = \min_{\omega} \{f^\Gamma\} \quad (13)$$

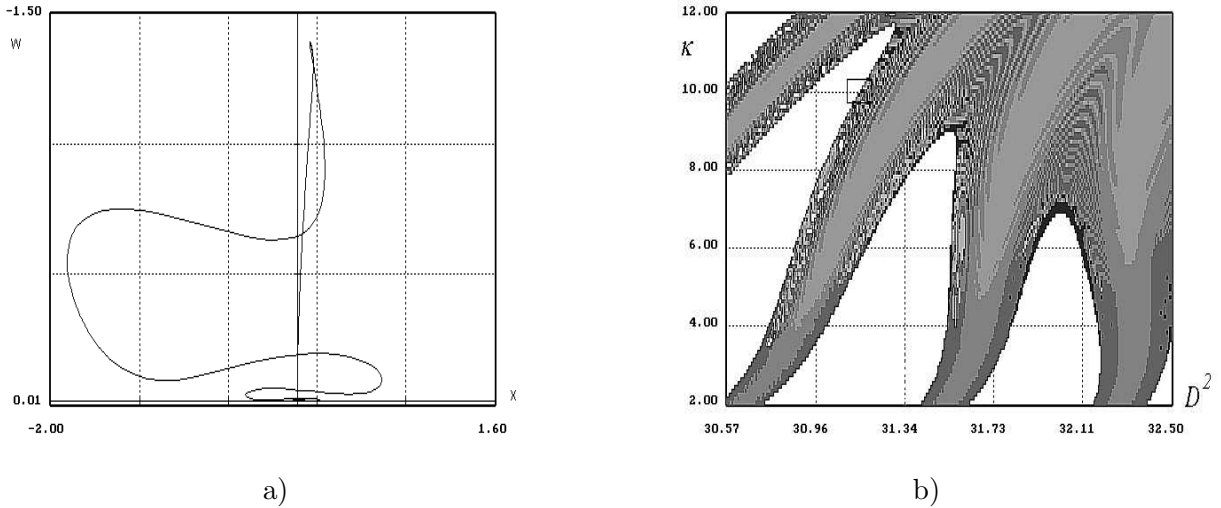


FIG. 3. a) Projection of the homoclinic solution of system (8) onto the (X, W) plane. b) A portrait of subset of parameter space (D^2, κ) , corresponding to different intervals of function $f_{\min}^{\Gamma}(D^2, \kappa)$ values and following Cauchy data: $X(0) = Y(0) = 0, W(0) = 0.001$: $f_{\min}^{\Gamma} > 1.2$ for white colour; $0.6 < f_{\min}^{\Gamma} \leq 1.2$ for light grey; $0.3 < f_{\min}^{\Gamma} \leq 0.6$ for grey; $0.01 < f_{\min}^{\Gamma} \leq 0.3$ for deep grey; $f_{\min}^{\Gamma} \leq 0.01$ for black.

for the part of the trajectory which lies beyond the point at which the distance gains its first local maximum, providing that it still lies inside the ball centered at the origin and having a fixed (sufficiently large) radius (for this case $f^{\Gamma}(\omega) \leq 5$). The results are presented in Figs.3b. The first is of the most rough scale among this series. Here, white color marks the values of parameters κ, D^2 for which $\Phi > 1.2$, light grey corresponds to the cases when $0.9 < \Phi < 1.2$ and so on (further explanations are given in the subsequent captions). The black coloured patches correspond to the case when $\Phi < 0.01$. In Ref. 14 the structure of the set of points from Fig. 3b has been studied in more detail.

IV. MODELS WITH DES TAKING SPATIAL AND TEMPORAL NONLOCALITIES INTO ACCOUNT

Combining the model (6) and (7), we obtain the following spatio-temporal nonlocal model

$$\tau(\dot{p} - \chi\dot{\rho}) = \kappa\rho - p + \sigma \left\{ p_{xx} + \frac{1}{\rho} p_x \rho_x - \eta \left(\rho_{xx} - \frac{1}{\rho} (\rho_x)^2 \right) \right\} - h \left\{ \ddot{p} + \eta \left(\frac{2}{\rho} (\dot{\rho})^2 - \ddot{\rho} \right) \right\}. \quad (14)$$

This model has been studied in Refs. 15 and 16, when the parameters h and σ are regarded as a small one, i.e., Eqs. (6) and (7) are perturbed by the terms with high derivatives. It turned out that the wave localized regimes are saved under perturbations and undergo some smooth changes.

V. MODELS INVOLVING DES WITH THE THIRD TEMPORAL DERIVATIVES

If we need to describe the relaxing processes in more detail, then we can incorporate the terms with the third temporal derivatives in DES (14). In this case DES has the form³

$$\begin{aligned} \tau \left(\frac{dp}{dt} - \chi \frac{d\rho}{dt} \right) &= \kappa\rho - p + \sigma \left\{ \frac{\partial^2 p}{\partial x^2} + \frac{1}{\rho} \frac{\partial p \partial \rho}{\partial x \partial x} - \chi \left(\frac{\partial^2 \rho}{\partial x^2} - \frac{1}{\rho} \left(\frac{\partial \rho}{\partial x} \right)^2 \right) \right\} - \\ &- h \left\{ \frac{d^2 p}{dt^2} + \chi \left(\frac{2}{\rho} \left(\frac{d\rho}{dt} \right)^2 - \frac{d^2 \rho}{dt^2} \right) \right\} + \frac{h^2}{\tau} \frac{d^3 p}{dt^3} + \frac{h^2 \chi}{\tau} \left\{ -\frac{6\dot{\rho}^3}{\rho^2} + \frac{6\dot{\rho}\ddot{\rho}}{\rho} - \frac{d^3 \rho}{dt^3} \right\}. \end{aligned} \quad (15)$$

Solutions (5) satisfy the following dynamical system

$$\begin{aligned} U \frac{dU}{d\omega} &= UW, \quad U \frac{dZ}{d\omega} = \gamma U + \xi Z + W(Z - U^2), \quad U \frac{dW}{d\omega} = UR, \\ U \frac{dR}{d\omega} &= (bU^3 (\chi - U^2))^{-1} \{ -\kappa U^2 + \eta \xi \sigma W - 2\xi \sigma U^2 W + \chi \tau U^2 W - h\xi U^4 W + \\ &+ b\xi^2 U^4 W - \tau U^4 W + \eta \sigma W^2 + (\chi h - \sigma) U^2 W^2 - hU^4 W^2 + b\xi U^4 W^2 - b\chi U^2 W^3 + \\ &+ bU^4 W^3 + \gamma (2\xi \sigma U + h\xi U^3 - b\xi^2 U^3 + \tau U^3 + 2\sigma UW) + U^2 Z + h\xi^2 U^2 Z - \\ &- b\xi^3 U^2 Z + \xi \tau U^2 Z + (-\eta \sigma U + U^3 \{ \sigma + \chi h - 4b\chi W - hU^2 + b\xi U^2 + 4bWU^2 \}) R \}, \end{aligned} \quad (16)$$

where $b = h^2/\tau$, and quadrature

$$U \frac{dS}{d\omega} = -(W + \xi).$$

The fixed point of this system has the coordinates

$$U_0 = -D, Z_0 = \frac{\kappa D^2}{D^2 - 2\sigma \xi^2}, W_0 = 0, R_0 = 0. \quad (17)$$

The conditions at which the linearized matrix \hat{M}

$$\hat{J} = \begin{pmatrix} 0 & 0 & a_1 & 0 \\ a_2 & a_3 & a_4 & 0 \\ 0 & 0 & 0 & a_5 \\ a_6 & a_7 & a_8 & a_9 \end{pmatrix} = \begin{pmatrix} 0 & 0 & -D & 0 \\ \gamma & \xi & Z_0 - D^2 & 0 \\ 0 & 0 & 0 & -D \\ a_6 & a_7 & a_8 & a_9 \end{pmatrix}, \quad (18)$$

$$\begin{aligned}
a_6 &= \frac{\kappa\xi(-2\xi\sigma + D^2(h\xi - b\xi^2 + \tau))}{\Delta D(2\xi^2\sigma - D^2)}, \quad a_7 = -\frac{1 + h\xi^2 - b\xi^3 + \xi\tau}{\Delta}, \\
a_8 &= -\frac{\xi\sigma(\eta - 2Z_0) - D^4(h\xi - b\xi^2 + \tau) + D^2(\chi\tau - 2\xi\sigma)}{D^2\Delta}, \\
a_9 &= \frac{\chi D^2 h - D^4 h + b D^4 \xi + D^2 \sigma - \eta \sigma}{D\Delta}, \quad \Delta = bD(\chi - D^2) \text{ admits the spectrum } (\pm\Omega^2 i; -\alpha_1; -\alpha_2)
\end{aligned}$$

have the form

$$B_2 = \frac{B_1}{B_3} + B_0 \frac{B_3}{B_1}, \quad B_3^2 - 4B_0 \frac{B_3}{B_1} \geq 0, \quad (19)$$

where $B_3 = -a_3 - a_9$, $B_2 = a_3 a_9 - a_5 a_8$, $B_1 = a_5(a_3 a_8 - a_1 a_6 - a_4 a_7)$, $B_0 = a_1 a_5(a_3 a_6 - a_2 a_7)$ are the coefficients of characteristic polynomial for the matrix \hat{M} .

If we fix the parameters $\chi = \eta = 30$, $\xi = -1.9$, $h = 1$, $\tau = 1$, $b = 1$, $\sigma = 2.7$, then in the plane (D^2, κ) Eq. (19) defines the NSC. Crossing this curve in the point $A(2.2852; 3.7)$, one can observe the appearance of the limit cycle at $D^2 \geq 2.2852$.

In the Poincaré diagram depicted at increasing D^2 (Fig.4) we can identify the moments of several period doubling bifurcations leading to the chaotic attractor creation. But the chaotic attractor existing at a short interval of parameter D^2 is destroyed. Instead of it in the phase space of system (16) the complicated periodic trajectory resembling to a loop (Fig. 5a) appears.

Consider also the development of oscillating regimes whose basins of attraction are separated from the basin of attraction of the main limit cycle. Integrating dynamical system (16) from initial conditions $(0; 0; 0; 0.01)$ at $D^2 = 2.722$, we see that the phase space of the system, in addition to the main limit cycle, contains the complicated trajectory (Fig. 5,a) which can be regarded as a hidden attractor. From the analysis of Poincaré diagram (Fig. 6a) it follows that the system weakly responds to the growing of the parameter D^2 until $D^2 = 2.7445$. When $D^2 > 2.7445$, the system jumps to another type of oscillations followed by chaotic regime creation.

If we plot the Poincaré diagram at decreasing D^2 (Fig. 6b) starting from the chaotic attractor, then we observe the periodic trajectory (Fig.5b) that differs from the initial regime (Fig.5a). Note that the periodic trajectory from Fig. 5b can be revealed directly by the integration from the initial conditions $(0; 0; 0; 0.1)$.

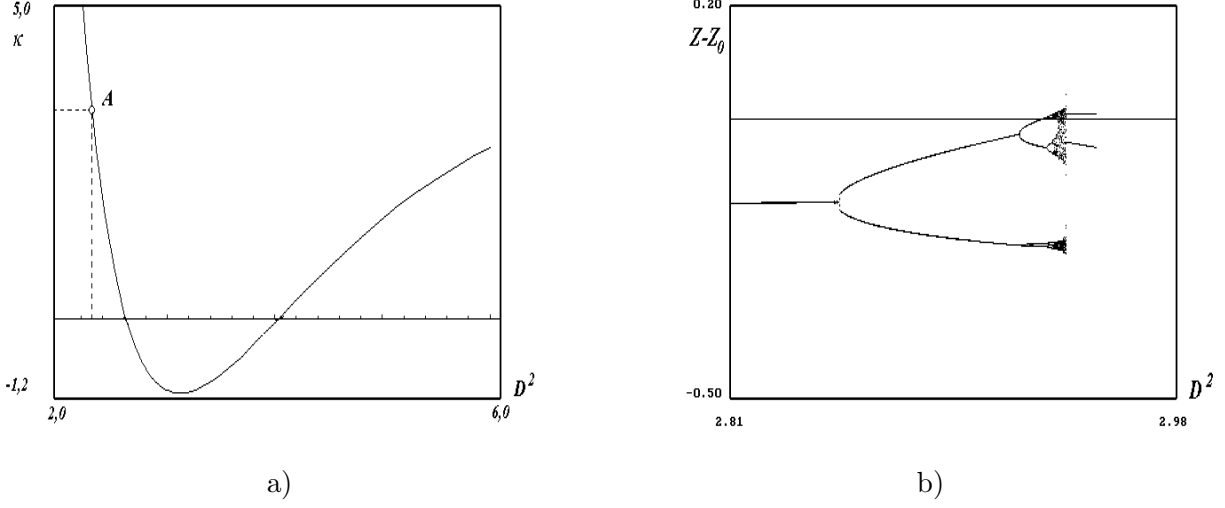


FIG. 4. a) Neutral stability curve in the plane $(D^2; \kappa)$. b) The bifurcation Poincaré diagram at increasing D^2

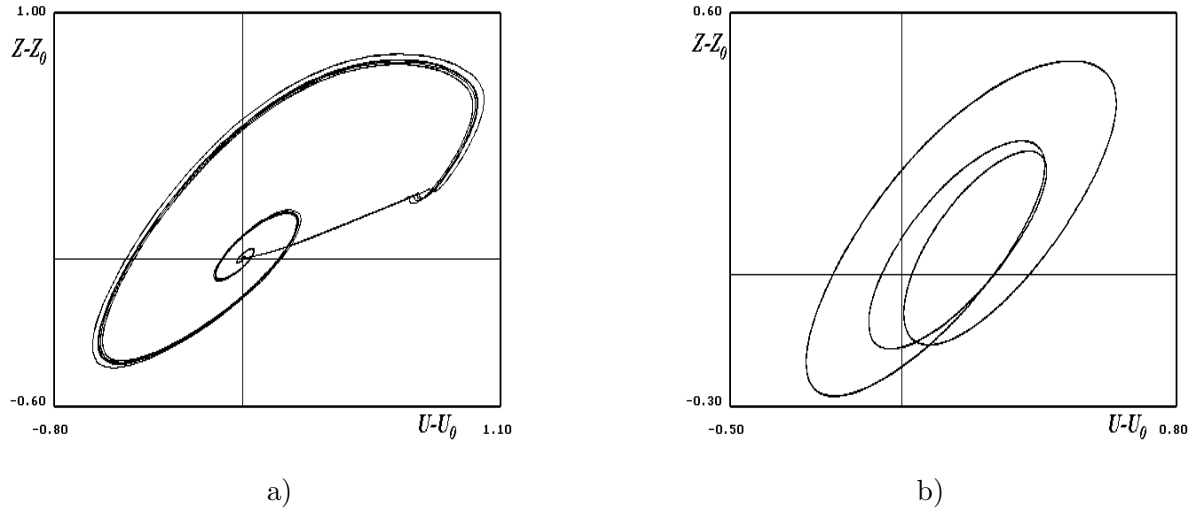


FIG. 5. Phase portraits of separated trajectories derived at $D^2 = 2.722$, $\kappa = 3.7$, $b = 1$ and different initial conditions.

VI. DES WITH PHYSICAL NONLINEARITY AND SECOND DERIVATIVES

Till now we dealt with the models without physical nonlinearity. Generalizing the previous models in this direction, we obtain the following model¹⁰

$$\sigma \chi \rho^{-2} \left[-\rho_{xx} (1 + a) + \rho_x^2 \rho^{-1} (1 - na) \right] +$$

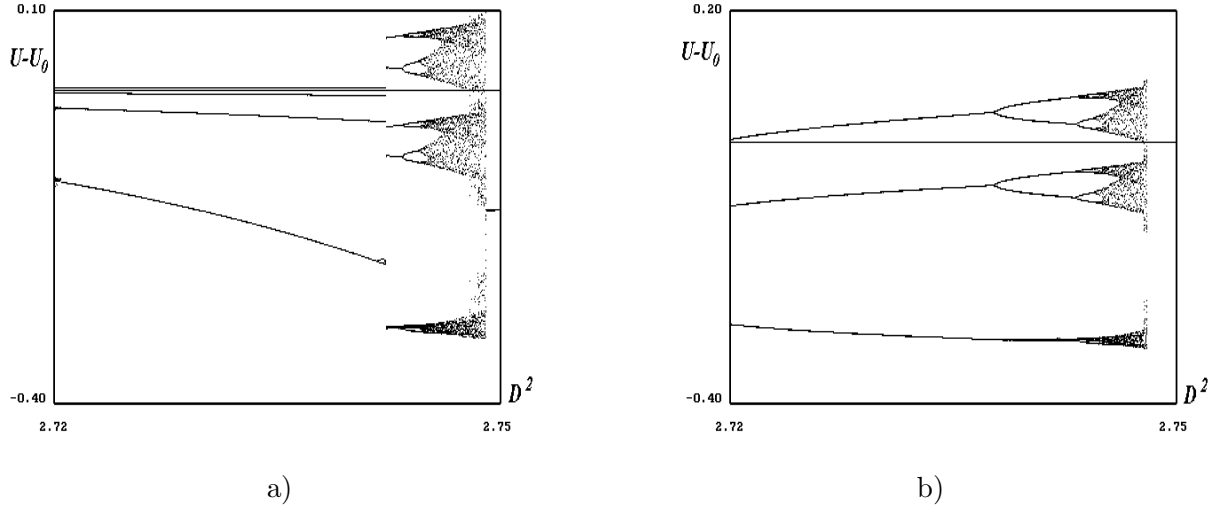


FIG. 6. The bifurcation Poincaré diagram of development of separated regime at increasing D^2 (a) and decreasing D^2 . Here $b = 1$.

$$\begin{aligned}
 +h\chi\rho^{-2}[-\ddot{\rho}(1+a) + 2\dot{\rho}^2\rho^{-1}(1 - 0.5a(n-1)) + \tau h^{-1}\dot{\rho}(1+a)] + \kappa\rho^n = p + \quad (20) \\
 +\tau\dot{p} - h\ddot{p} - \sigma(p_{xx} + \rho_x p_x \rho^{-1}), \quad a = \delta n \rho^{n+1}.
 \end{aligned}$$

Properties of solutions to system (20) can be found out using the symmetry of the system with respect to the Galilei group⁶. One can be persuaded by direct verification that system (20) allows operator

$$\hat{X} = \frac{1}{2\xi} \frac{\partial}{\partial t} + t \frac{\partial}{\partial x} + \frac{\partial}{\partial u}.$$

Let us construct an ansatz with its invariants

$$\rho = R(\omega), \quad p = P(\omega), \quad u = 2\xi t + U(\omega), \quad \omega = x - \xi t^2, \quad (21)$$

where parameter ξ is proportional to acceleration of the wave front. Substitution (21) into the system yields the following quadrature

$$UR = C = \text{const}$$

and the dynamical system

$$\begin{aligned}
R' &= W, \quad P' = \gamma R^m - 2\xi R + \frac{C^2}{R^2}W, \\
W' &= -(\kappa R^{n+3} - PR^3 - P'R^2C\tau - hP'C^2W + P'R^2\sigma W + \\
&+ \gamma m R^{2+m}\sigma W + \chi L\tau CW + \gamma hm R^m C^2W + h\chi L(CWR^{-1})^2 - \\
&- 2C^2\sigma W^2 + \chi M\sigma W^2 - 2C^4hR^{-2}W^2 + \\
&+ 2h\chi NC^2R^{-2}W^2 - 2R^3\sigma W\xi - 2hRC^2W\xi) \times \\
&((C^2 - \chi L)R(\sigma + hC^2R^{-2}))^{-1},
\end{aligned} \tag{22}$$

where $(\cdot)' = \frac{d}{d\omega}(\cdot)$, $L = 1 + a$, $M = 1 - an$, $N = 1 - 0.5a(n - 1)$, $a = \delta n R^{n+1}$.

The single isolated equilibrium (neglecting the trivial) point has the following coordinates

$$R_0 = \left(\frac{2\xi}{\gamma}\right)^{1/m-1}, \quad P_0 = \kappa R_0^n, \quad W_0 = 0. \tag{23}$$

In this point the linearized matrix \hat{M} has the form

$$\hat{M} = \begin{pmatrix} 0 & 0 & 1 \\ a_1 & 0 & a_2 \\ a_3 & a_4 & a_5 \end{pmatrix}, \tag{24}$$

where

$$\begin{aligned}
a_1 &= 2\xi(n-1), \quad a_2 = C^2R_0^{-2}, \\
a_3 &= (2C^3h[C^2 - \chi L]\tau[\gamma R_0^m - 2\xi R_0]R_0^{-2} + \\
&+ C\chi(n+1)(L-1)\tau\Delta - C[C^2 - \chi L]\tau\Delta - \\
&- [C^2 - \chi L](C^2hR_0^{-2} + \sigma)(\kappa n R_0^{1+n} - C\tau(\gamma(2+m)R_0^m - 6\xi R_0)))/\Delta^2, \\
a_4 &= R_0^2\Delta^{-1}, \\
a_5 &= \frac{C^2\gamma h(nR_0^n - R_0^m) - C^3\tau + C\chi L\tau + R_0^2\sigma(\gamma[R_0^m + nR_0^n] - 4R_0\xi)}{R_0\Delta}, \\
\Delta &= (C^2 - \chi L)(C^2hR_0^{-2} + \sigma).
\end{aligned}$$

The NSC for system (22) has the following form

$$G(\xi, \sigma, n, h, \tau, \kappa, \chi) \equiv a_5(a_3 + a_2a_4) + a_1a_4 = 0. \tag{25}$$

Let us make the values of parameters fixed as follows:

$$\gamma = 1, \quad \chi = 10, \quad C = -2.8, \quad \sigma = 0.2, \quad \tau = 1.1, \quad h = 3.2, \quad \delta = 1.4, \quad n = m = 3.2.$$

Condition (25) allows us to find numerically the value of $\xi_0 = 0.157$ corresponding to birth of the limit cycle.

Let us consider in more detail the influence on the revealed regimes of parameters n and δ changes, which determine nonlinearity of the medium in the dynamic equation of state. Let us make the value of parameter $\xi = 0.35$ fixed, in case of which there is a limit cycle with period $2T$ in the space of the system.

The diagram reveals some peculiarities of system's (22) behavior. In particular, we would like to pay attention to the presence of a "special" point in the parameter plane, surrounded by four different types of solutions. One can also see the "windows" of periodicity (area 6) among the chaotic area. To find out the structure of phase space in more detail near area 6 of Fig.7a, let us plot a one-parametric Poincaré diagram (Fig.7b) for $\delta = 1.4$ and a decrease of parameter n .

In case of n close to 2, abrupt reconstruction of the chaotic attractor structure can be observed, which is probably caused by the interaction of two (or more) co-existing attractors of a dynamic system. In case of $n \approx 1.4$ the chaotic trajectory is localized in a more narrow area of phase space of system (22), stipulating the appearance of a specific window of periodicity with a decrease of n . Analysis of a two-parametric bifurcation diagram for the value of parameter $\kappa = 2$ (Fig.7a) shows that the area of existence of the chaotic attractor increases and the windows of regular intervals in case of the increasing κ shift towards higher values of the nonlinearity parameter n .

A crucially different set of bifurcations is observed in case of a change of parameter σ .

Let us fix the values of parameters $\gamma = 1$, $\chi = 10$, $C = -2.8$, $\tau = 1.1$, $\kappa = 0.9$, $h = 3.2$, $\xi = 0.35$, $n = m = 3.2$ and $\delta = 0.4$. Integrating system (22) with initial data $(0, 0, 0.01)$ and $\sigma = 5$ within phase space near the equilibrium point, in addition to the limit cycle, other periodic trajectory has been found with a separated pool of attraction (development of this regime with increasing of σ is presented in Fig.7b graph II).

The presence of such a regime leads to the thought of the existence of quasi-periodic regimes. To look for such a regime let us plot a bifurcation diagram of Poincaré for development of basic limit cycle in case of increasing parameter σ (Fig.7b graph I).

Another bifurcation, leading to the appearance of the toroidal surface, has been discovered in this system. An intersection of the toroidal attractor with the plane $y_3 = 0$ forms a closed curve, shown in Fig.8a. A further increase of parameter σ causes the synchronization of tore

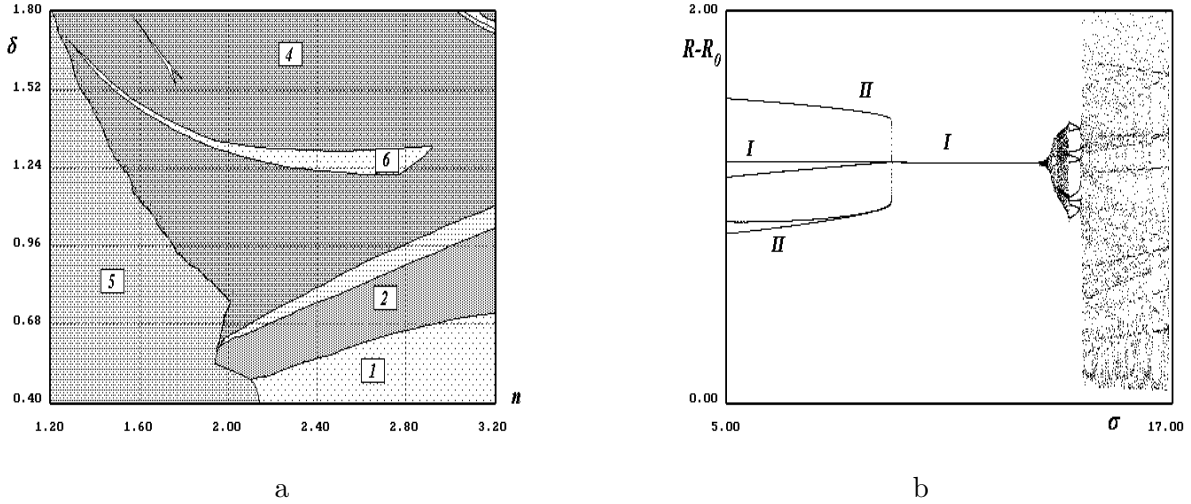


FIG. 7. a) Two-parametric bifurcation diagram in case of $\kappa = 2$ (for other values of parameters and conventional symbols see Fig.3; b) Poincaré bifurcation diagram for development of the torus in case of $\gamma = 1$, $\chi = 10$, $C = -2.8$, $\tau = 1.1$, $\kappa = 0.9$, $h = 3.2$, $\delta = 0.4$, $\xi = 0.35$, $n = m = 3.2$ and increasing σ , where graph I is the basic limit cycle, graph II – complicated periodic trajectory with separated region of attraction.

frequencies, and finally an abrupt increase of vibrations amplitude, which shows the creation of a crucial new dynamical behavior. To clarify the character of the produced regime, let us analyze the Poincaré section for the case of $\sigma = 14.6$ (Fig.8b). The plotted cross-section is specific for chaotic attractor, which provides reasons for statements on the existence of bifurcation of a quasi-periodic regime with a producing chaotic attractor.

It turned out that system (22) provides another type of chaotic attractor creation, namely, intermittency. Let us fix $\gamma = 1$, $\chi = 50$, $C = -1.5$, $\tau = 0.1$, $\kappa = 1.9$, $\sigma = 0.2$, $h = 0.9$, $\xi = 0.18$.

Plotting the Poincaré bifurcation diagram (Fig. 9a), we see that a limit cycle undergoes several period doubling bifurcations resulting in the chaotic attractor creation. But the development of chaotic attractor is interrupted suddenly and new complicated periodic trajectory appears which bifurcates in chaotic attractor as well at increasing n . Considering the hereditary sequences (Fig.9b) for chaotic trajectories, we found that the graph of the map $W_{i+1} = f(W_i)$ is close to the bissectrice at $n = 4.25$. As in the case with the Lorentz system, existence of narrow passage leads to the alternation of the chaotic and regular behavior of the system trajectories.

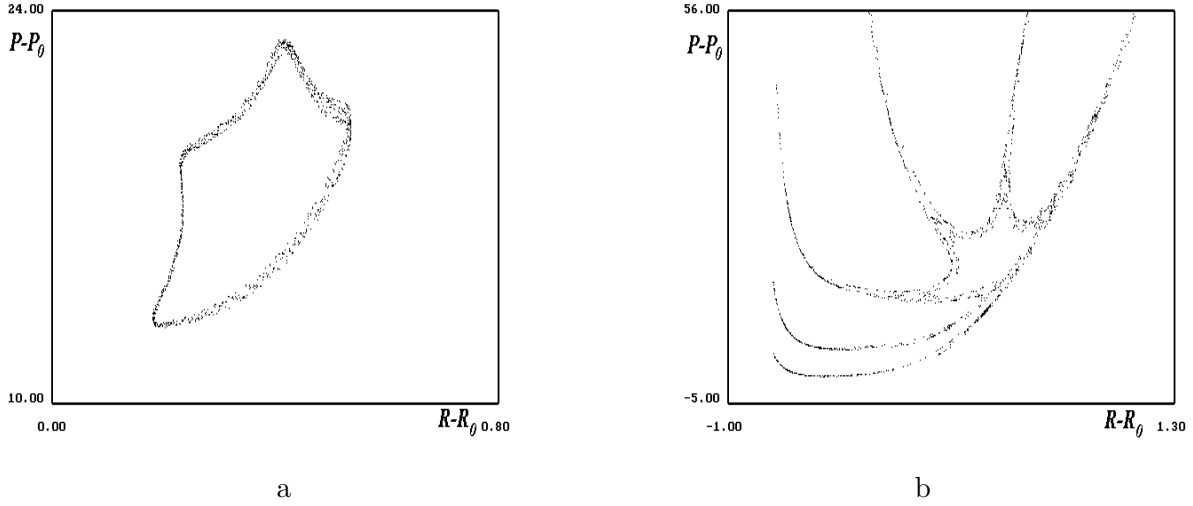


FIG. 8. a) The Poincaré cross-section of the torus surface in case of $\sigma = 14$ b) The Poincaré cross-section of a chaotic attractor in case of $\sigma = 14.6$. Fixed parameters $\gamma = 1$, $\chi = 10$, $C = -2.8$, $\tau = 1.1$, $\kappa = 0.9$, $h = 3.2$, $\delta = 0.4$, $\xi = 0.35$, $n = m = 3.2$.

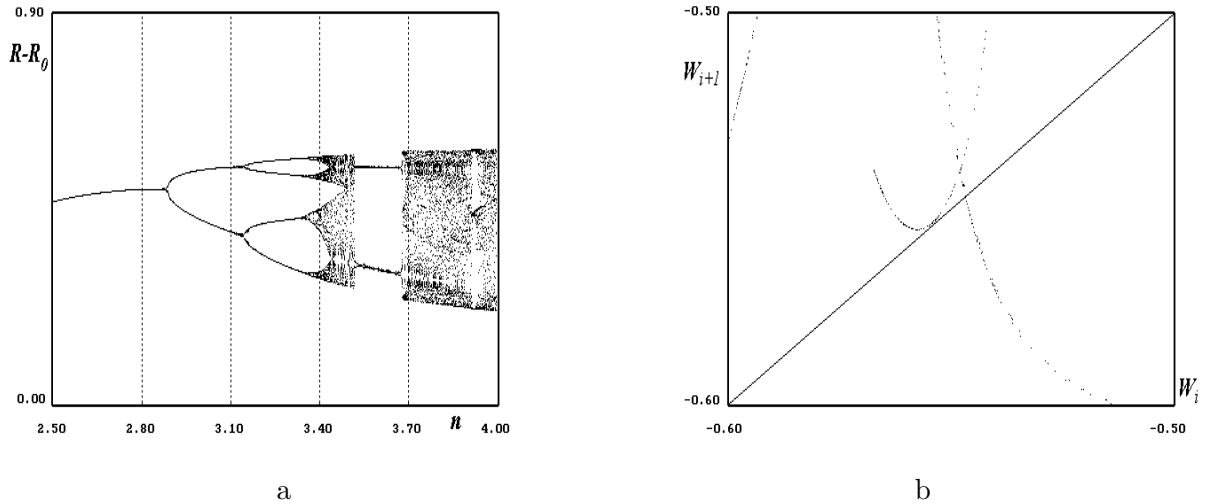


FIG. 9. a) The bifurcation diagram at increasing n . b) The graph of dependence W_{i+1} vs W_i at $n = 4.25$. The fixed values of parameters $\gamma = 1.49$, $\chi = 50$, $C = -1.5$, $\tau = 0.1$, $\kappa = 1.9$, $\sigma = 0.2$, $h = 0.9$, $\xi = 0.18$, $\delta = 0.8$.

VII. CONCLUSIONS

Finally, we have studied the hierarchical sequences of the mathematical models for non-equilibrium media. Analyzing the wave fields in such media we have shown that derived models possess the wide set of localized wave regimes. In particular, the models with relax-

ation admit the periodic, multiperiodic, chaotic solutions. Spatially nonlocal models have in addition quasiperiodic and solitary wave solutions. All the models demonstrate the most bifurcations and scenarios of chaotic regimes creation.

From the other hand, identifying internal variables with parameters undergoing fluctuations, one can consider these investigations as the problem on the dissipative structures creation under the influence of noise.

REFERENCES

- ¹V. A. Vladimirov, V. A. Danylenko, and V. Y. Korolevych, “Nonlinear models for multi-component relaxing media: dynamics of wave structures and qualitative analysis,” Preprint (Subbotin Institute of Geophysics, 1990) in Ukrainian.
- ²T. B. Danevych and V. Danylenko, “Governing equations for nonlinear media with internal variables taking temporal and spatial nonlocalities into account,” Preprint (Subbotin Institute of Geophysics, 1999) in Ukrainian.
- ³T. B. Danevych, V. A. Danylenko, and S. I. Skurativskiy, *Nonlinear mathematical models of media with temporal and spatial nonlocalities* (Subbotin Institute of Geophysics, 2008).
- ⁴V. A. Danylenko, V. V. Sorokina, and V. A. Vladimirov, *Journal of Physics A* **26**, 7125–7135 (1993), DOI:10.1088/0305-4470/26/23/047.
- ⁵V. A. Vladimirov, *Opuscula Mathematica* **23**, 81–94 (2003).
- ⁶V. I. Lahno, S. V. Spichak, and V. I. Stogniy, *Symmetry analysis of evolution type equations* (Computer Research Institute, Moscow–Igevsk, 2004).
- ⁷V. N. Sidorets and V. A. Vladimirov, “On the peculiarities of stochastic invariant solutions of a hydrodynamic system accounting for non-local effects,” in *Symmetry in Nonlinear Mathematical Physics*, 2, edited by M. Shkil, A. Nikitin, and V. Boyko (Institute of Mathematics, Kyiv, 1997) pp. 409–417.
- ⁸J. Guckenheimer and P. Holmes, *Nonlinear oscillations, dynamical systems and bifurcations of vector fields* (Springer–Verlag, New York, 1987).
- ⁹M. Holodniok, A. Klić, M. Kubiček, and M. Marek, *Methods of Analysis of Nonlinear Dynamical Models* (World Publishing House, Moscow, 1991).
- ¹⁰V. A. Danylenko and S. I. Skurativskiy, *Rep. Math. Phys.* **59**, 45–51 (2007), DOI:10.1016/S0034-4877(07)80003-6.

- ¹¹N. V. Butenin, J. I. Neimark, and N. A. Fufaev, *Introduction to the theory of nonlinear oscillations* (Nauka, Moscow, 1987).
- ¹²S. Wiggins, *Introduction to applied nonlinear dynamical systems and chaos* (Springer-Verlag, New York, 1990).
- ¹³Y. A. Kuznetsov, *Elements of applied bifurcation theory* (Springer-Verlag, New York, 1998).
- ¹⁴V. A. Vladimirov and S. I. Skurativskiy, Rep. Math. Phys. **46**, 287–294 (2000), DOI: 10.1016/S0034-4877(01)80034-3.
- ¹⁵V. A. Vladimirov, V. A. Danylenko, and S. I. Skurativskiy, Reports of NAS of Ukraine **12**, 104 – 108 (2004).
- ¹⁶S. I. Skurativskyy, Nonlinear Phenom. Complex Syst. **4:4**, 390–396 (2001).